Crystal structure, electric and magnetic properties in Na$_x$CoO$_2$

K.Nagasawa and H.Nakatsugawa

Division of Materials Science and Engineering, Graduate School of Engineering, Yokohama National University
79-5 Tokiwadai, Hodogaya Ward, Yokohama 240-8501 Japan
Fax: +81-45-331-6593, e-mail: naka@ynu.ac.jp

The electron density distributions of γ -Na$_x$CoO$_2$ have been obtained by the maximum entropy method and the Rietveld analysis using synchrotron radiation X-ray diffraction data at 100K, 200K and 300K. In the Rietveld refinement, the deviation of (008) and (108) peaks is very large relative to that of other reflections with increase of Na content x. And same behavior showed by the change of temperature. Electron density distribution based on synchrotron radiation X-ray diffraction data showed the direct observation of the formation of the Co$-$O hybridization with increasing the Na content. This means increase of covalency between O $2p$ and Co t_{2g} in the CoO$_2$ layer. But not showed the change of electron density distribution between 100K and 300K. These facts indicate the essential difference for respective cause of the peak deviation.

Key words: γ -Na$_x$CoO$_2$, Synchrotron radiation X-ray diffraction, Maximum Entropy Method

1.INTRODUCTION

Recently, a layered cobalt oxide Na$_x$CoO$_2$ have been known as a promising candidate for thermoelectric materials because of its large thermoelectric power (S) coexisting with low electric resistivity (ρ).[1] The carrier concentration has been found to be much higher in this system, i.e., the order of $10^{21} \sim 10^{22}$ cm^{-3}, than in some known thermoelectric materials such as Bi$_2$Te$_3$ and PbTe.[2] The large value reported for S of Na$_{0.5}$CoO$_2$, i.e., S >50 μ V/K at room temperature, is difficult to be understood within the framework of conventional one-electron picture.[3] A recent result of heat capacity measurements [4] revealed that the effective mass of the carrier (holes) of this compound was as large as those of strongly correlated electrons. Terasaki [3] suggested that both the strong electron correlation and the spin sate in Co site play a crucially important role in the enhancement of S. The magnetic susceptibility (χ) of polycrystalline sample of Na$_{0.5}$CoO$_2$ was successfully explained by the coexistence of Co^{3+} (low-spin: t_{2g}^6) and Co^{4+} (low-spin: t_{2g}^5). [5] Koshibae et al. [6] established a theory generalizing the Heikes' formula [7] and suggested that the observed large magnitude of S in Na$_x$CoO$_2$ would be originated from both the large degeneracy of Co species of various spin states and the strong correlation of $3d$ electrons. It was concluded that the low-spin state in Co site is a key factor for the large Seebeck coefficient.

The structure of the material is of a layer type consisting of CdI$_2$-type CoO$_2$ conducting layers which are made of edge-shared CoO$_6$ octahedra and interlayers of Na$^+$ ions alternately stacked along the c-axis. The sodium ions are intercalated in trigonal prismatic or octahedral coordination of oxygen atoms and are mobile even at room temperature, but the ionic conductivity is much smaller than the electronic conductivity in the CoO$_2$ layers. Delmas et al. [8] have reported that Na$_x$CoO$_2$ has four distinct bronze-type phases, i.e., α (O3-type structure), α '(O'3-type structure), β (P3-type structure), and γ (P2-type structure), and the difference among these four phases is in the stacking sequence of oxygen atom layers. The neutron diffraction investigation [9] of Na$_{0.74}$CoO$_2$ has shown that the material has a hexagonal γ phase (space group: $P6_3/mmc$, No.194) and that there are two types of Na$^+$ sites, i.e., $2b$ (0, 0, 1/4) and $2d$ (2/3, 1/3, 1/4), with different occupancies. The $2d$ site is in a trigonal prismatic environment, while the $2b$ site has neighboring Co ions above and below the trigonal prism of the oxygen atom, which should cause the difference in the occupancy. Such a disordered structure also should cause a low thermal conductivity, i.e., 20mW/cmK at room temperature, which was attributed to the short phonon mean free path arising from the Na deficiency. [10] Na$_x$CoO$_2$ is known to show a wide range of Na nonstoichiometry within $0.5 \leq x \leq 1.0$, where the valence of Co changes Co$^{3+}_x$Co$^{4+}_{1-x}$ in accordance with Na$^+$ content x. Since Na is volatile, it has been recognized that the control of x is difficult for Na$_x$CoO$_2$ by a conventional solid state reaction method. [11]

Recently, however, Motohashi et al. [12,13] established an unconventional method named rapid heat-up (RH) technique to precisely control the sodium content in Na$_x$CoO$_2$ samples, in which Na evaporation during the synthesis is minimized. For thus prepared samples of Na$_{0.75}$CoO$_2$ exhibit $S \sim 120 \mu$ V/K at room temperature, [12] and show a magnetic transition of the second order below 22K. [13] These features strongly indicate the appearance of an unusual electronic state that may be attributed to strongly correlated electrons in Na$_{0.75}$CoO$_2$. Furthermore, Tojo et al. [14] measured the heat capacity of Na$_{0.75}$CoO$_2$ and found first order phase transitions at 288.7, 296.3, and 302.1K. The x-ray diffraction patterns in Na$_{0.75}$CoO$_2$ at 123 and 333K indicate that the most probable mechanism of the phase transition around room temperature is the occurrence of some kind of ordering in Na$^+$ layers. [14] Although a large number of studies have been made on the strongly

correlated electron system in the CoO$_2$ layers, little is known about a relationship between the CoO$_2$ layers and the Na$^+$ layers. Thus, a further investigation is needed to confirm these clearly. From this point of view, the magnetic properties, the parameters of the crystal structure, and the charge density distributions visualized by a combination of the maximum entropy method (MEM) and a Rietveld refinement [15,16] in Na-richer samples by a conventional solid state reaction method have been investigated in the present study.

2.EXPERIMENTAL PROCEDURE

Polycrystalline samples γ -Na$_x$CoO$_2$ were prepared by the RH technique [12,13] to precisely control the sodium content. Starting powders of Na$_2$CO$_3$ and Co$_3$O$_4$ were mixed with an appropriate molar ratio (x=0.73, 0.75, 0.77, 0.79, 0.81 and 0.83). Because of reduce impurities, samples ware calcined two times at 1153K for 12h in air. Then, the samples were reground, pressed into pellets and sintered at 1193K for 12h in air. Finally, the pellets were cooled in the furnace to room temperature at a rate of 1K/min. The resulting powder sample was characterized by X-ray diffraction (XRD) and synchrotron radiation x-ray diffraction. Each the X-ray pattern showed good identification of the samples as the γ phase, and there was no indication of the presence of other prototypes or residual raw materials.

The XRD measurement was carried out using a JEOL JDX-3530 x-ray diffractometer system at room temperature. The powder samples were pressed on a glass plate, mounted vertically on the sample table and diffraction patterns are recorded using CuKα (λ =1.54 Å) radiation. The XRD data is collected in 2theta range from 10 to 90° in steps of 0.02° using a scintillation detector. The same samples were carried out the synchrotron radiation X-ray diffraction on the Large Debye-Scherrer Camera installed at BL02B2 for high efficiency and high resolution measurements in Spring-8 by Japan Synchrotron Radiation Research Institute (JASRI). The temperatures were performed at 100K, 200K, and 300K by the N$_2$ gas flow system. The sample was sealed into quartz capillary of 0.2mm in diameter. An incident X-ray wavelength was 0.50Å.

The structure determination of γ -Na$_x$CoO$_2$ was analyzed using the Rietveld analysis program, RIETAN-2000. [17] The charge density distributions at 100K, 200K and 300K were visualized by an elaborate method, which are combination of the MEM and the Rietveld refinement of the X-ray diffraction data. [15,16] Moreover, magnetic susceptibility (χ) was measured between 5K and 300 K using a commercial apparatus from Quantum Design MPMS superconducting quantum interference device (SQUID) magnetometer.

3.RESULTS AND DISCUSSION

The synchrotron radiation powder X-ray data showed that the samples (x=0.73, 0.75, 0.77, 0.79, 0.81 and 0.83) were single phase and had the P2-type hexagonal structure, where the highest symmetry *P6$_3$/mmc* type space group (No.194) was chosen as it described the refined structure equally. [9] In Figs.1,2 the results of the Rietveld refinement are shown for (I) x=0.75 and

(II) x=0.81 at (a)300K, (b)200K and (c)100K. In the present analysis we assumed that Na1 and Na2 ions occupy *2b* (0,0,1/4) and *2d* (2/3,1/3,1/4) sites, respectively. The weighted profile reliability factors of the Rietveld refinement as a pre-analysis for the MEM, R_{wp}, were (I -a) 8.36%, (I -b) 8.48%, (I -c) 8.38%, (II -a) 7.09%, (II -b) 7.17% and (II -c) 7.17%. There are good agreement between the results of the Rietveld refinement, except for two peaks, i.e., (008) (2theta$\fallingdotseq$ 21.3°) and (108) (2theta$\fallingdotseq$24.5°). It should be noted that (112) and (202) reflections deviate to low 2theta angle side, but (008) and (108) reflections deviate to high 2theta angle side with increasing x. Furthermore, the similar behavior was continuously observed as it cooled to low temperature in all samples. Considering the change of diffraction pattern accompanying increase of Na content x and cooling temperature, the decrease of lattice parameter c causes the deviation of (008) and (108).

(I) (a)

(I) (b)

(I) (c)
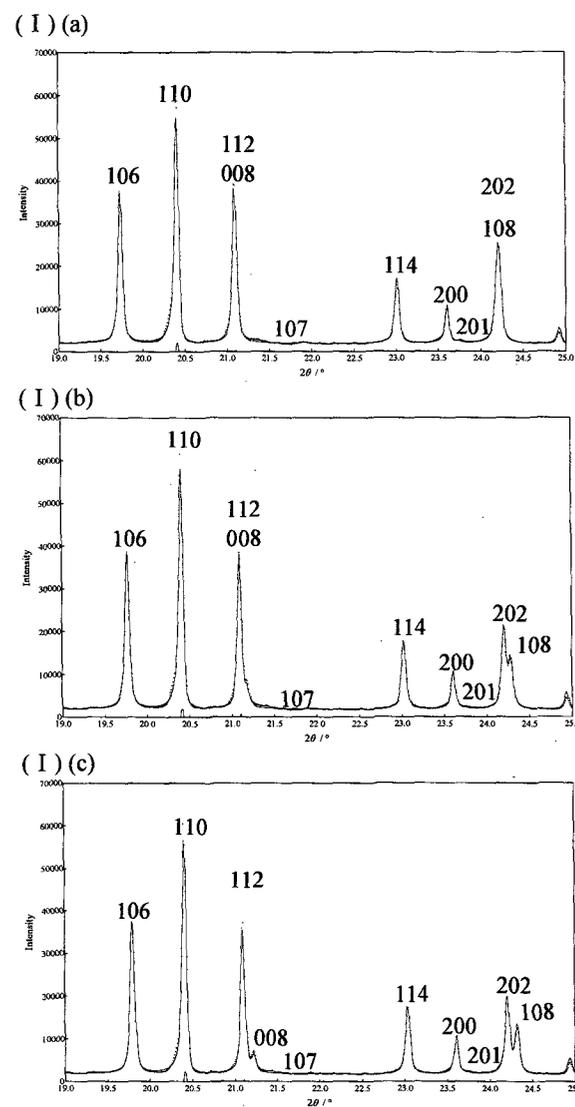
Fig. 1. Rietveld fitting pattern of synchrotron radiation powder X-ray data at (a)300K, (b)200K and (c)100K for (I) x=0.75.

(Ⅱ) (a)

(Ⅱ) (b)

(Ⅱ) (c)
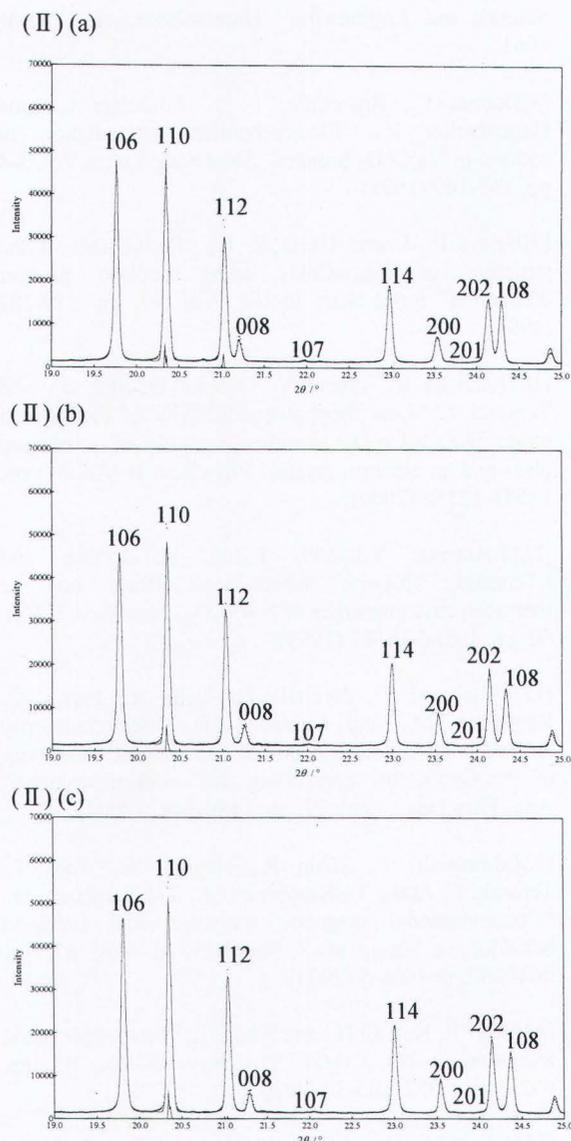
Fig. 2. Rietveld fitting pattern of synchrotron radiation powder X-ray data at (a)300K, (b)200K and (c)100K for (Ⅱ)ʹx=0.81.

The number of observed synchrotron radiation X-ray diffraction structure factors derived in the Rietveld analysis was 255 for each set of data, which were used for further MEM analysis. Following the Rietveld analysis, the MEM analysis was carried out with a computer program, MEED, [18] using $50 \times 50 \times 100$ pixels. In the MEM imaging, any kind of deformation of electron densities is allowed as long as it satisfies the symmetry requirements. This method enables us to visualize more detailed features included in the observed data like the bonding electron distribution associated with hybridized orbital.

In Figs.3, the three-dimensional representation of the MEM charge densities for samples of (a) x=0.75 and (b) x=0.81 together with the MEM charge densities in the (002) plane for both samples. An equi-contour surface is drawn only for the lower density region. In these figures, there are Co-O network of the electron density for x=0.81, but no significant network for x=0.75 in

equi-counter surface (ⅰ) 1.5 e/$Å^3$. This is the direct observation of increase of the Co-O hybridization in the CoO_2 layer with increasing the sodium content from x=0.75 to 0.81. In particular, the change in the electron density distribution should be attributed to the decrease of the lattice parameter c with increasing x. Understanding from the MEM imaging, increase of Na content induces the binding between Na+ ions. Consequently, interaction between Na layers and CoO_2 layers is decrease. This is also understudied that electron density of Co ions changed between x=0.75 and x=0.81 in equi-counter surface (ⅱ) 2.0 e/$Å^3$. In a word, the Co-O hybridization and the decrease of the lattice parameter c cause the interaction in *a-b* plane direction. But the change of electron density distribution between 100K and 300K is not showed. This is simply that the decrease of the lattice parameter c caused by the thermal contraction.

(Ⅰ) (a) (ⅰ)   (Ⅰ) (a) (ⅱ)

(Ⅰ) (b) (ⅰ)   (Ⅰ) (b) (ⅱ)

(Ⅱ) (a) (ⅰ)   (Ⅱ) (a) (ⅱ)

(Ⅱ) (b) (ⅰ)   (Ⅱ) (b) (ⅱ)
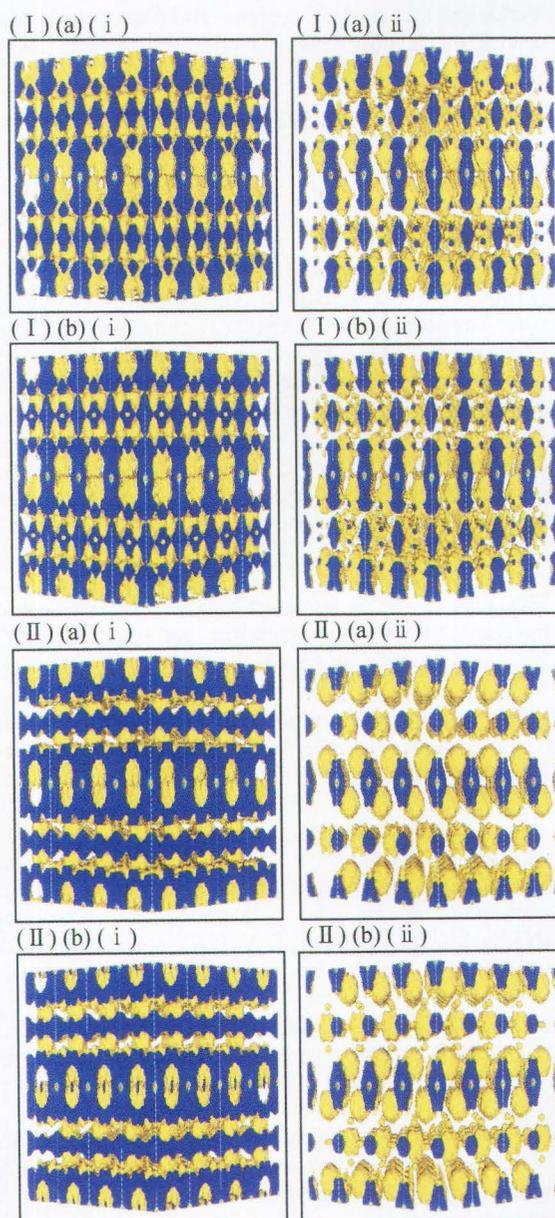
Fig. 3. Three-dimensional representation of the MEM

charge distribution at (a)300K and (b)100K for (I) x=0.75 and (II) x=0.81 [equi-contour surface (i) 1.5e/ Å^3 (ii) 2.0e/ Å^3]

4.CONCLUSION

The all samples were single phase and had the P2-type hexagonal structure (space group: $P6_3/mmc$, No.194) at 100K, 200k and 300K. In the present analysis we assumed that Na1 and Na2 ions occupy *2b* and *2d* sites, respectively. The sodium ions cannot fully occupy the adjacent *2b* and *2d* sites so that these are randomly distributed at the both sites with different occupancies. In the Rietveld refinement, there are good agreement between x=0.75 and x=0.81, except for (008) and (108) peaks. The deviation of the two reflections is very large relative to that of other reflections. Electron density distribution based on the synchrotron radiation X-ray diffraction data show the direct observation of increase of the Co-O hybridization in the CoO$_2$ layer with increasing the sodium content. But not showed the change of electron density distribution between 100K and 300K.

5.ACKNOWLEDGMENTS

6.REFERENCES

[1]Terasaki, I., Sasago, Y., and Uchinokura K., "Large thermoelectric power in NaCo$_2$O$_4$ single crystals" Phys.Rev B Vol. 56, pp. R12685-R12687 (1997).

[2]Mahan G., Sales B., and Sharp J., "Thermoelectric materials: new approaches to an old problem" Phys.Today Vol. 50, pp. 42-47 (1997).

[3]Terasaki I., *in Proceedings of the 18th International Conference on Thermoelectrics* (ICT1999), Baltimore, MD, Aug.29-Sept.2, 1999 (IEEE, Piscataway, 2000), pp. 569-576.

[4]Ando Y., Miyamoto N., Segawa K., Kawata T., and Terasaki I., "Specific-heat evidence for strong electron correlations in the thermoelectric material (Na,Ca)Co$_2$O$_4$" Phys.Rev. B Vol. 60, pp. 10580-10583 (1999).

[5]Ray R., Goshray A., Goshray K., and Nakamura S., "^{59}Co NMR studies of metallic NaCo$_2$O$_4$" Phys.Rev. B Vol. 59, pp. 9454-9461 (1999).

[6]Koshibae W., Tsutsui K., and Maekawa S., "Thermopower in cobalt oxides" Phys.Rev. B Vol. 62, pp. 6869-6872 (2000).

[7]Heikes R. R. and Ure R. W., Jr., Thermoelectricity: Science and Engineering (Interscience, New York, 1961).

[8]Delmas C., Braconnier J-. J., Fouassier C., and Hagenmuller P., "Electrochemical intercalation of sodium in Na$_x$CoO$_2$ bronzes" Solid State Ionics Vol. 3-4, pp. 165-169 (1981).

[9]Balsys R. J. and Davis R. L., "Refinement of the structure of Na$_{0.74}$CoO$_2$ using neutron powder diffraction" Solid State Ionics Vol. 93, pp. 279-282 (1996).

[10]Takahata K., Iguchi Y., Tanaka D., Itoh T., and Terasaki I., "Low thermal conductivity of the layered oxide (Na,Ca)Co$_2$O$_4$: Another example of a phonon glass and an electron crystal" Phys.Rev. B Vol. 61, pp. 12551-12555 (2000).

[11]T.Kawata, Y.Iguchi, T.Itoh, K.Takahata, and I.Terasaki, "Na-site substitution effects on the thermoelectric properties of NaCo$_2$O$_4$" Phys.Rev. B Vol. 60, pp. 10584-10587 (1999).

[12]Motohashi T., Naujalis E., Ueda R., Isawa K., Karppinen M., and Yamauchi H., "Simultaneously enhanced thermoelectric power and reduced resistivity of Na$_x$Co$_2$O$_4$ by controlling Na nonstoichiometry" Appl.Phys.Lett. Vol. 79, pp. 1480-1482 (2001).

[13]Motohashi T., Ueda R., Naujalis E., Tojo T., Terasaki I., Atake T., Karppinen M., and Yamauchi H., "Unconventional magnetic transition and transport behavior in Na$_{0.75}$CoO$_2$" Phys.Rev. B Vol. 67, pp. 064406-1-064406-5 (2003).

[14]Tojo T., Kawaji H., and Atake T., "First-order phase transition in Na$_{1.5}$Co$_2$O$_4$" Phys.Rev. B Vol. 65, pp. 0521105-1-0521105-3 (2002)

[15]Takata M., Umeda B., Nishibori E., Sakata M., Saito Y., Ohno M., and Shinohara H., "Confirmation by X-ray diffraction of the endohedral nature of the metallofullerene Y@C$_{82}$" Nature Vol. 377, pp. 46-49 (1995).

[16]Takata M., Nishibori E., Umeda B., Sakata M., Yamamoto E., and Shinohara H., "Structure of endohedral dimetallofullerene Sc$_2$@C$_{84}$" Phys.Rev.Lett. Vol. 78, pp. 3330-3333 (1997).

[17]Izumi F. and Ikeda T., "A Rietveld-Analysis Program RIETAN-98 and its Applications to Zeolites" Mater. Sci. Forum Vol. 321-324 pp. 198-203 (2000).

[18]Kumazawa S., Kubota Y., Takata M., Sakata M., and Ishibashi Y., "MEED: a program packae for electron-density-distribution calculation by the maximum-entropy method" J.Appl.Crystallogr. Vol. 26, pp. 453-457 (1993).